

Radar Cross Section Analysis for Frequency Selective Surface Radome based on SBR Method

S. Kuroda*, Y. Inasawa, S. Morita, H. Nishikawa and Y. Konishi
Mitsubishi Electric Corporation
5-1-1 Ohfuna, Kamakura, Kanagawa 247-8501, Japan
shinkuro@isl.melco.co.jp

1. Introduction

The purpose of this paper is to show an analysis method for a radar cross section (RCS) of targets with the radome composed of frequency selective surface (FSS). The FSS radome is widely used on many airplanes and ships [1] in order to reduce RCS. For RCS of the radome, several analysis methods have been reported based on the method of moments (MoM) [2]-[4]. Clearly, these methods can analyze the RCS of the FSS radomes. However, these methods have to use large computer memory and large calculation time when applying actual size radomes. On the other hands, we have studied an analysis method based on the shooting and bouncing rays (SBR) method [5] for such problems [6].

In this paper, we propose the simple analysis method based on the SBR method for analyzing the RCS of the target with FSS radomes.

2. Analysis Procedure

The procedure of analysis proposed here is as follows:

- (1) We derive reflection and transmission characteristics of the FSS. These parameters can be calculated by applying the MoM.
- (2) The scattered field of the target (scatterer and FSS radome) can be obtained by the SBR method. The above parameters are used as the reflection and transmission coefficients of the radome on ray tracing.

The reflection and transmission characteristics of FSS can be obtained as follows [7]:

- (I) We expand the electric fields using the vector Floquet modes.
- (II) We obtain the reflected and transmitted fields by solving the simultaneous integral equations using the MoM.
- (III) We derive the reflection and transmission coefficients by normalizing with the incident field.

After obtaining the reflection and transmission coefficients, we can calculate the total backscattered field based on SBR method by using these coefficients on ray tracing. The detail procedure of the derivation is described in [6].

3. Experiment

We perform the monostatic RCS experiment for the test target to verify the proposed analysis method. For the experiment, we have prepared two types of FSS, named "FSS1" and "FSS2". Figure 1 shows the summary of the surface element pattern of the FSS1 and FSS2. FSS1 consists of the periodic dielectric ring shape elements on the metallic plate, while FSS2 consists of the periodic dielectric cross shape elements on the metallic plate. We summarize the electric characteristics of the dielectrics in Table 1. Fig.2 shows the section structure of the FSSs. Fig. 3 shows configuration of the test target, consists of the FSS plate on the aperture of metallic trihedral corner reflector (TCR). The aperture is being kept perpendicular to the X axis and the bottom side is parallel to the Y axis.

Figs. 4 and 5 show frequency characteristics and RCS angular pattern at 10GHz of the TCR with FSS1, respectively. The incident and observation direction is the same, $\theta = 90$ deg. and $\phi = 0$ deg. Both the measured and calculated components of the electrical fields are theta components E_θ . The radome aperture of the test target is being kept perpendicular to the ground (X-Y plane). The solid line and dashed line denote the measured and calculated RCS values respectively. In Fig.4, clear difference between calculated and measured data can be observed above 11GHz. On the contrary, the calculated and measured data of the angular pattern in Fig.5 are in good agreement.

Figs. 6 and 7 show frequency characteristics and RCS angular pattern at 10GHz of the TCR with FSS2, respectively. The incident and observation direction is the same, $\theta = 90$ deg. and $\phi = 0$ deg. Both the measured and calculated components of the electrical fields are phi components E_{ϕ} . In Fig.6, the calculated and measured data are in good agreement except for the difference of resonant frequency. Similarly, the calculated and measured data of the angular pattern in Fig.7 are in good agreement.

4. Conclusions

The authors proposed the simple analysis method for target with radome composed of FSS based on the SBR method. Also, the authors confirmed effectiveness of this method for the FSS radomes by the experiment.

References

- [1] E. F. Knott, J. F. Shaeffer and M. T. Tuley, Radar cross section second edition, Artech house publishers, Boston, 1993.
- [2] E Arvas and S. Ponnappalli, "Scattering cross section of a small radome of arbitrary shape," IEEE Trans. Antennas and Propagat., vol.37, no.5, pp.655-658, May 1989.
- [3] S. S. Bindiganavale, J. L. Volakis and H. Wang, "Dielectric nose radome scattering by using the fast multipole method to calculate the RCS of large objects," IEEE Antennas and Propagat. Symp. Digest, no.6, pp.930-933, June 1996.
- [4] W. J. Zhao, L. W. Li and Y. B. Gan, "Application of adaptive integral method to scattering analysis of arbitrary shaped radomes," Proceedings of 2002 Interim International Symposium on Antennas and Propagation, pp.153-156, Nov. 2002.
- [5] H. Ling, R. Chou and S. Lee, "Shooting and bouncing rays: Calculating the RCS of an arbitrarily shaped cavity," IEEE Trans. Antennas and Propagat, vol.37, no.2, pp.194-205, Feb. 1989.
- [6] S. Kuroda, Y. Inasawa, Y. Konishi and S. Makino, "Radar Cross Section Analysis Considering Multi-Reflection inside a Radome Using SBR Method," IEEE Antennas and Propagat. Symp. Digest, no.4, pp.4503-4506, June 2004.
- [7] J. P. Montgomery, "Scattering by an infinite periodic array of thin conductors on a dielectric sheet," IEEE Trans. Antennas and Propagat., vol.AP-23, no.1, pp.70-75, Jan. 1975.

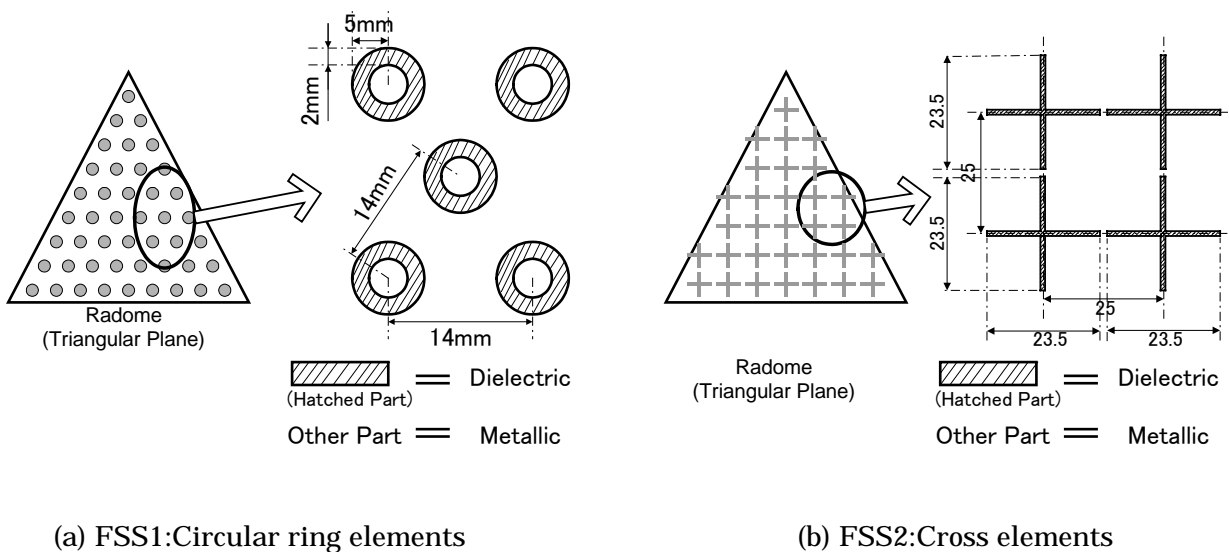


Fig. 1: Summary of the FSS radome.

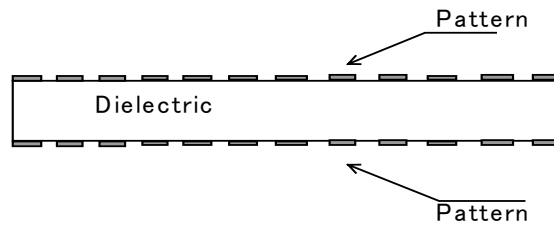


Fig. 2: Sectional structure of the FSS1 and FSS2.

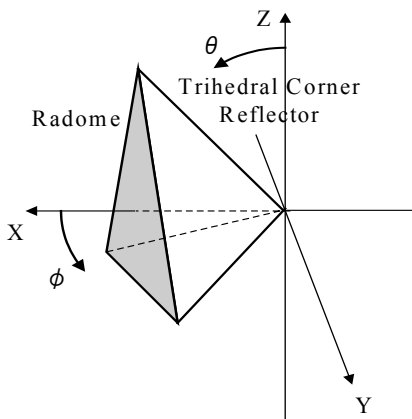


Fig. 3: Test target configuration.

Table. 1: Electric Characteristics of the dielectric of FSS.

Parameter	FSS1	FSS2
Permittivity	3.55	2.60
Dissipation Factor	0.003	0.002
Thickness	4.0mm	1.6mm

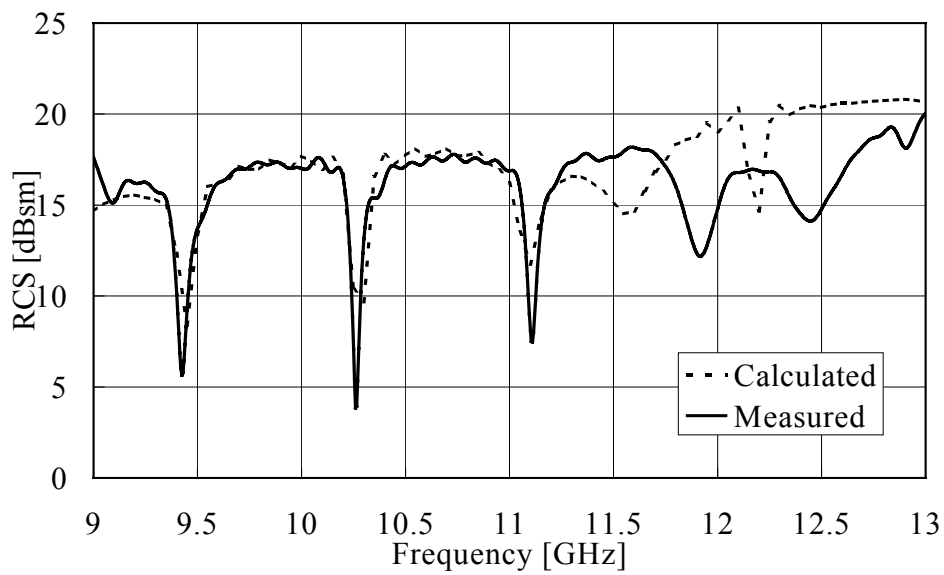


Fig. 4: Frequency characteristics of the reflector with the radome of FSS1.

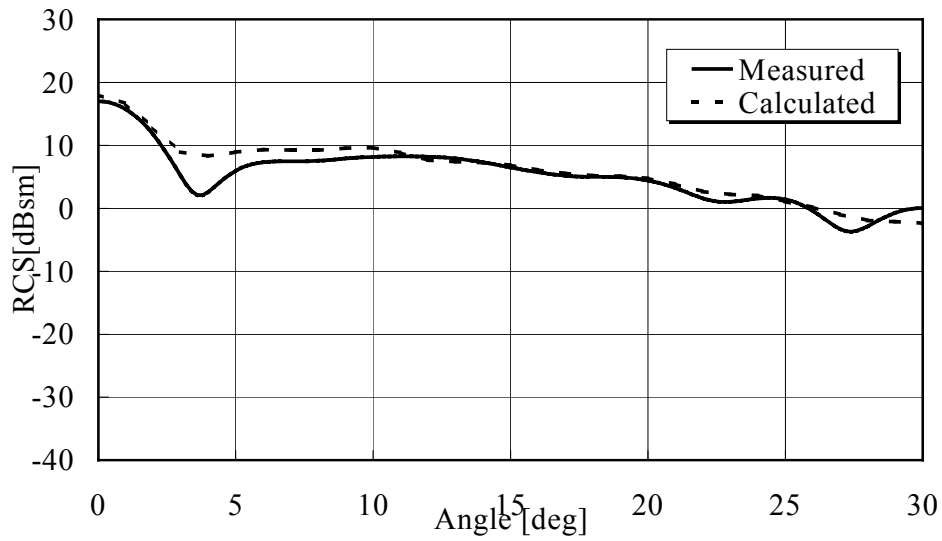


Fig. 5: RCS angular pattern of the reflector with the radome of FSS1.

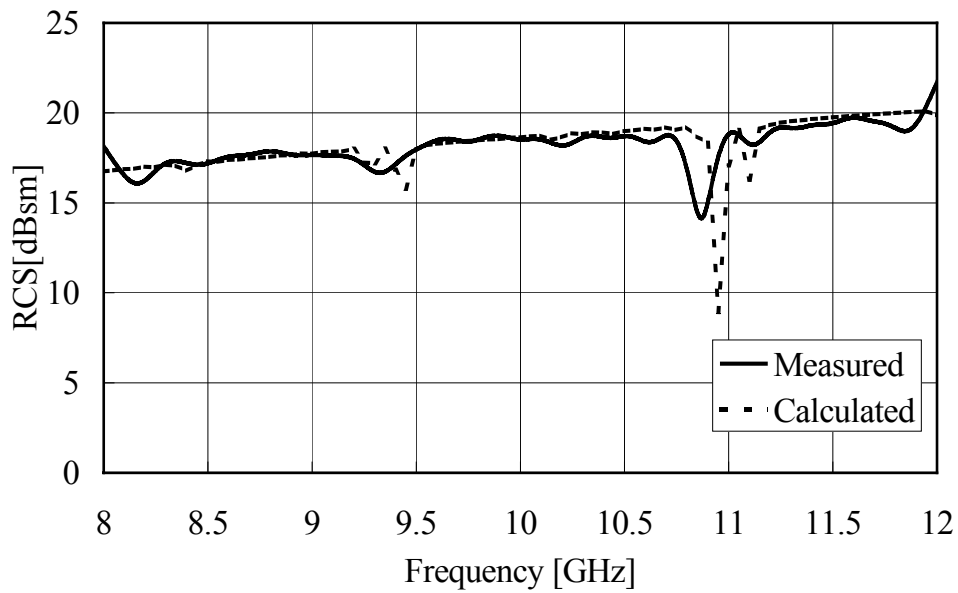


Fig. 6: Frequency characteristics of the reflector with the radome of FSS2.

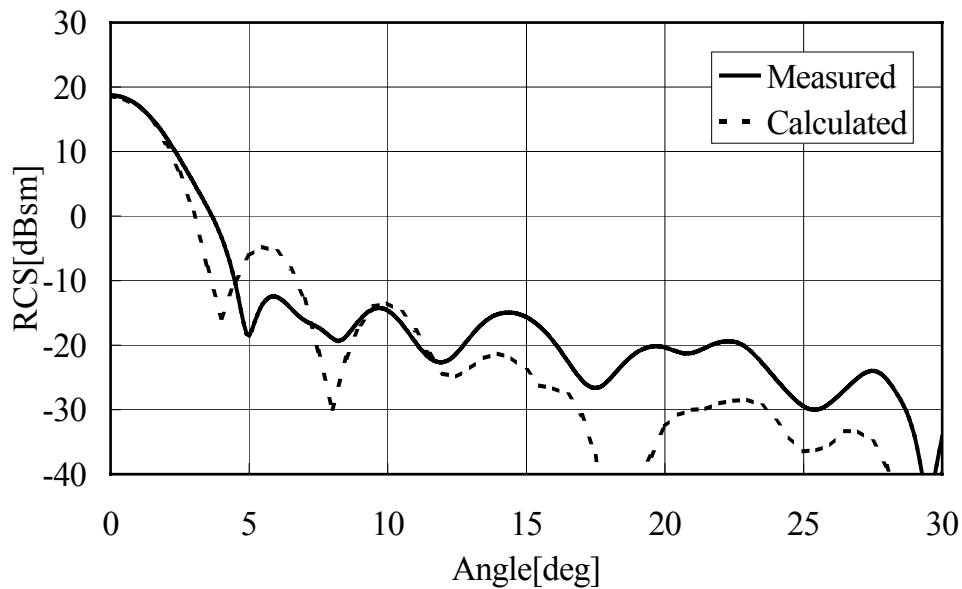


Fig. 7: RCS angular pattern of the reflector with the radome of FSS2.